ELSEVIER

Journal of Nuclear Materials 271&272 (1999) 184–188

journal of nuclear materials

Section 12.3. Microstructural evolution

Defect-flow-induced heterogeneous dislocation formation and solute redistribution near a grain boundary in austenitic stainless steel under electron irradiation

S. Watanabe [a,*], N. Sakaguchi [b], S. Mochizuki [b], H. Takahashi [b]

[a] *Department of Materials Science, Faculty of Engineering, Hokkaido University, Sapporo 060, Japan*
[b] *Center for Advanced Research of Energy Technology, Hokkaido University, Sapporo 060, Japan*

Abstract

The authors investigated radiation-induced segregation (RIS) at a grain boundary in an Fe–Cr–Ni alloy under irradiation taking account of the evolution of faulted dislocation loops and network dislocations. Electron irradiation with a high voltage electron microscope (1000 kV) at Hokkaido University, Japan, was performed to study radiation-induced solute segregation and point defect flow in a typical austenitic Fe–Cr–Ni alloy. The theoretical analysis was conducted by solving the coupled rate equations for solute and defect concentrations near a grain boundary sink. The experimental solute redistribution profiles predicted by the theory were explained qualitatively. The formation of dislocation free zone (DLFZ) in the vicinity of a grain boundary was also observed during in situ observation under electron irradiation. The temperature dependence of the segregation width and that of DLFZ zone width show similar trends. It is thus suggested that RIS and DLFZ formation should be explained by the defect-flow-induced phenomenon under irradiation. The inter-relationship between RIS and such heterogeneous defect clustering near a grain boundary was also clarified substantially.

1. Introduction

It is well-known that many kinds of phenomena occur in materials during irradiation with high energy particles such as neutrons, electrons and/or ions. Important radiation-induced phenomena include radiation-induced segregation (RIS), radiation-enhanced diffusion, radiation-induced precipitation, radiation-induced grain boundary migration and/or radiation-induced amorphization as well as microstructural changes. These radiation-induced phenomena are known to be closely related to the point defects introduced due to collision between high energy particles and atoms in an alloy.

Among these phenomena, the RIS near grain boundaries is known to cause a significant degradation in physical, chemical and/or mechanical properties [1] in an alloy such as type 316 stainless steel, which has been considered as the primary candidate for structural materials of near-term fusion reactors and which is used as light-water reactor core components [2,3]. It is thus of great importance to investigate retardation of radiation induced solute redistribution [4–7].

On the other hand, a defect-free zone (DFZ) has been known to occur near the grain boundary. Some examples are the formation of precipitation free zone (PFZ) or, so-called, denuded zone under thermal aging [8], of void free zone [9] and of helium bubble free zone [10], under irradiation. Such heterogeneous microstructural formation of defect clusters near a grain boundary is commonly understood in terms of the interrelation between the diffusional process of the supersaturated impurities or point defects, i.e., vacancies and interstitials, toward the grain boundary sink and the subsequent microstructural evolution process that vicinity. An exceptional case is the DFZ formation by deformation, which has been observed not near a grain boundary but in a matrix during deformation followed by quenching or irradiation [11].

* Corresponding author. Fax: +81-11 757 3537; e-mail: watanabe@bloch.metall.hokudai.ac.jp

0022-3115/99/$ – see front matter
PII: S0022-3115(98)00778-8

The main purpose of the present paper is to experimentally investigate RIS at a grain boundary in an austenitic Fe-Ni-Cr alloy accompanied by DLFZ formation as a consequence of heterogeneous dislocation evolution during electron irradiation [12]. We used in-situ observation with a high voltage electron microscope (1 MV) and compared the results with the prediction by computer simulation discussed by Sakaguchi et al. [13].

2. Experimental and computational methods

Specimens of an Fe–15Cr–20Ni alloy containing 20.1 Ni, 15.2 Cr and, as impurities, 0.003 C and 0.0011 N (in wt%) were used. After heat treatment at 1323 K for 60 min and electro-polishing, the thin foil TEM specimens were irradiated with 1 MeV electrons at various temperatures using a high voltage electron microscope. The mean damage rate was 1.0×10^{-3} dpa/s. The temperatures and doses were in the ranges of 523–623 K and 1.0–10.0 dpa, respectively, which are the conditions where RIS and DLFZ formation are easily observed. After irradiation, we carried out ion-thinning of the TEM specimen with an ion-milling instrument (GATAN: DuoMill Model 600) for a few minutes, in order to get rid of surface regions of a few hundred nano-meters, and then the chemical composition was determined using a conventional analytical 200 kV transmission electron microscope (JEOL-2000FX) equipped with an energy dispersive X-ray analyzer.

The details of the simulation are in a previous paper by Sakaguchi et al. [13]. In the calculation, we also considered the spatial resolution in the EDS analysis with a finite-size probe, by means of averaging the calculated concentration profile by the formula of normalized two dimensional Gaussian average for the one dimensional concentration profile [7]. The probe radius, R, used in averaging was 10 nmat a given dose for a conventional TEM and for a 200 nm-thick stainless steel sample. The last technique is necessary for simulating the actual profile data obtained by TEM-EDS analysis.

3. Results and discussion

3.1. Microstructure change and DLFZ formation during irradiation

In Fig. 1 we show DLFZ formation and its change observed during electron irradiation near a random grain boundary in a Fe–15Cr–20Ni at temperature of 523 K and at damage rate of 1.0×10^{-3} dpa/s. The DLFZ, white regions at the both sides of the grain boundary in the photos, formed at the first stage as the dislocation loop formation occurred and became visible with a width of about 30 nm at 0.4 dpa, then it narrowed as the dose increased further. The loops are well known faulted interstitial Frank-type loops with the Burgers vector of $a/3\ \langle 1\ 1\ 1\rangle$ and unfaulted type loops with $a/2\ \langle 1\ 1\ 0\rangle$ [11]. There were also some network dislocations evolved during irradiation. Although not visible in the photos, a small number of void-like clusters, probably stacking fault tetrahedra, were observed at the higher dose and at a different view. Almost no defects are, however, observed in the DLFZ region.

We show in Fig. 2 the dose dependence of the DLFZ width, W_{DLFZ}, change at 523 K as a function of electron dose. Each width datum point is plotted as an average of ten measurements of DLFZ widths relative to the grain boundary. The solid line in the figure corresponds to the theoretical prediction by the computational method of Sakaguchi et al. [13]. Neglecting minor deviations

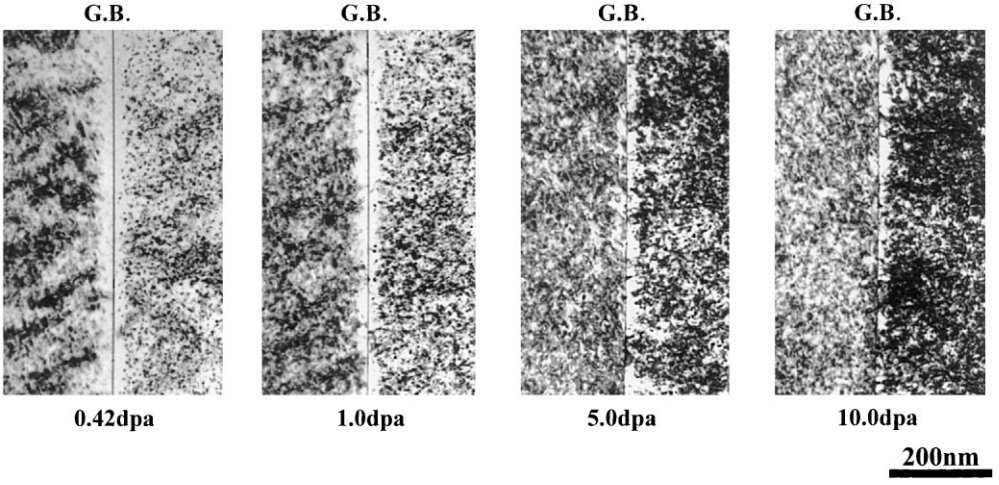

Fig. 1. Dose dependence of DLFZ near a grain boundary in a Fe–15Cr–20Ni alloy electron irradiated at 1×10^{-3} dpa/s and at 523 K.

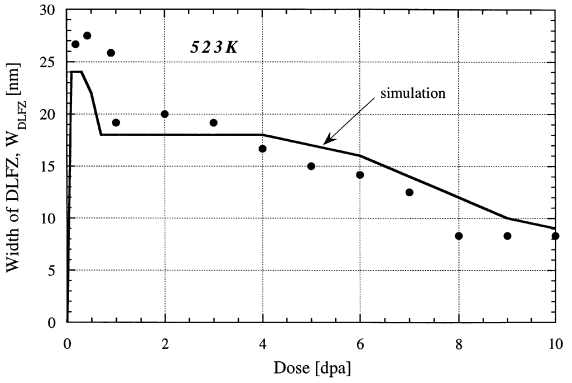

Fig. 2. Dose dependence of DLFZ width: experimentally observed in HVEM (filled circles) and theoretical prediction (solid line).

between the experimental and simulated results, overall agreement was obtained. The feature of dose dependence of DLFZ width can be described as follows.

It showed an abrupt decrease around 1 dpa after a constant period and then a gradual decrease. The theoretical consideration indicates that this corresponds to the build up of supersaturated point defects and also to the initial RIS saturating behavior (around 1 dpa).

3.2. Temperature dependence of DLFZ formation and RIS

The temperature dependence of the DLFZ formation in one Fe–15Cr–20Ni alloy at a dose of 0.6 dpa electron irradiation is shown in Fig. 3. As the temperature increased the loop density decreased but the size of each loop became large and the width of the DLFZ was then enlarged. The values of widths, W_{DLFZ}, at 1.0 dpa were 15, 30 and 63 nm at 523, 573 and 623 K, respectively. We show in Fig. 4 corresponding theoretical and experimental results on RIS near the grain boundaries in Fig. 3. The theoretical results (solid lines) agree well with the data at the all temperatures examined. In Fig. 4 W_{DLFZ} and W_{RIS} defined as the local minima in Ni's (also maxima in Cr's) profiles, viz., the characteristic segregation distance, are shown indicated by arrows. Fig. 5 shows the relationship between the segregation width and the DLFZ width to be linear. This linearity has also been supported by theory [13]. The slope, however, will increase as dose increases because W_{RIS} is enlarged and W_{DLFZ} in Fig. 2 decreases at higher doses.

3.3. Analytical discussion and formation energy of DLFZ

In Fig. 6 we plotted W_{DLFZ} as a function of the inverse of temperature with the simulation results. The previous experimental data in Section 3.2 are shown by the triangles and the lower solid line is the theoretical prediction on W_{DLFZ}. The upper line in the figure is the theoretical result for the solute diffusivity under irradiation, which can be defined as the summation form of partial diffusivity multiplied by each point defect concentrations:

$$D_{\mathrm{s}}^{\mathrm{irr}} = d_{\mathrm{sv}} C_{\mathrm{v}}^{\mathrm{irr}} + d_{\mathrm{si}} C_{\mathrm{i}}^{\mathrm{irr}} \equiv D_{\mathrm{s}}^{0} \exp\left(-\frac{E^{\mathrm{irr}}}{kT}\right), \tag{1}$$

where $D_{\mathrm{S}}^{\mathrm{irr}}$ and E^{irr} are the solute diffusivity and the activation energy of solute-diffusion under irradiation and $D_{\mathrm{s}}^{0} = \exp(S^{\mathrm{f}}/k)\exp(-E^{\mathrm{f}}/kT)$ under the usual definitions [7]. In this temperature region the $D_{\mathrm{S}}^{\mathrm{irr}}$ for Ni is linear in the Arrhenius plot. Although the Cr diffusivity shows almost the same dependence, the faulted loop may usually contain a large number of Ni interstitial atoms; thus the subscript s can be thought as Ni solute. From the slope analysis we can see that the formation energy of the DLFZ is half of the activation energy of solute diffusivity. The experimental value of Q was 0.4 ± 0.1 eV.

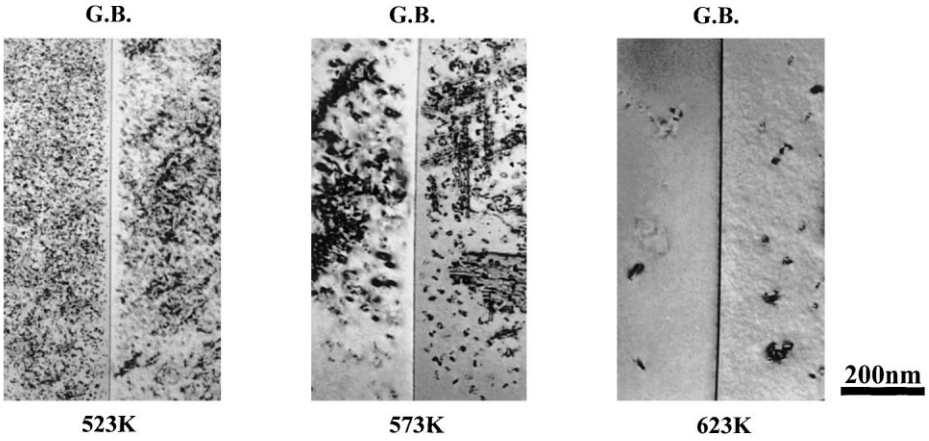

Fig. 3. Temperature dependence of DLFZ formation at 0.6 dpa.

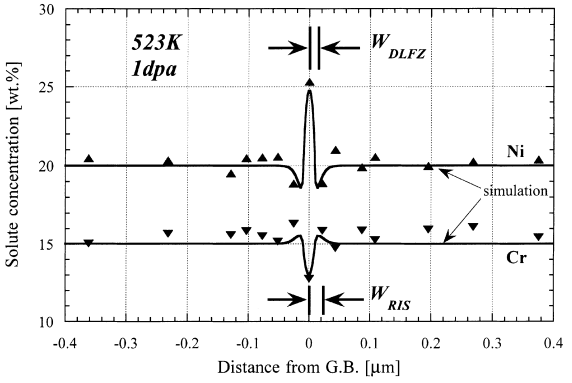

Fig. 4. Solute concentration profiles after electron irradiation to 1 dpa: W_{RIS} is a segregation width and W_{DLFZ} is the DLFZ width. Solid lines are for the theoretical RIS prediction.

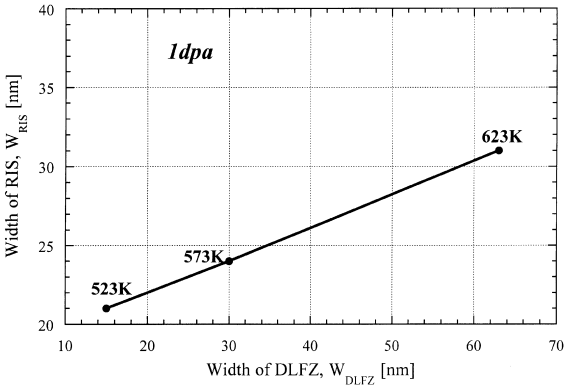

Fig. 5. A relationship between DLFZ width and RIS width (experimental results).

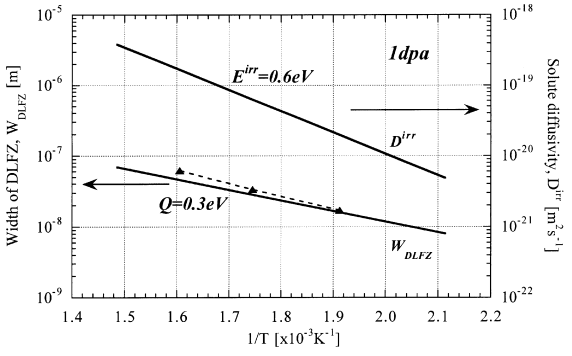

Fig. 6. Arrhenius plots of D^{irr} for Ni and W_{DLFZ}: theory (solid lines); experiment (triangles).

From Fig. 5 we can see that the RIS and DLFZ formation are related to the same thermally activated process. At a given time the characteristic diffusion length is given by

$$\text{Diffusion length} \propto \sqrt{D}. \tag{2}$$

Analogously, we expect under irradiation that DLFZ width is proportional to RIS width with the square root of the diffusivity, i.e.,

$$W_{DLFZ} \propto W_{RIS}$$

$$\propto \sqrt{D_s^{irr}} \quad \text{(from Fig. 5 and Eq. (2))} \tag{3}$$

$$\propto \exp\left(-\frac{E^{irr}/2}{kT}\right) \quad \text{(from Eq. (1))}. \tag{4}$$

Hence, *the formation energy in the DLFZ, Q, is the half of migration energy, E^{irr}, in radiation-enhanced solute diffusion. i.e.,*

$$Q = \frac{E^{irr}}{2}. \tag{5}$$

4. Concluding remarks

The authors investigated radiation-induced segregation and heterogeneous microstructure through dislocation free zone formation near a grain boundary under irradiation. It can be said about the DLFZ formation and the RIS that the supersaturated point defects, i.e., vacancies and interstitials, introduced during irradiation dominantly diffuse to a grain boundary sink and a DLFZ forms near the grain boundary where there in no secondary defect formation. After the extra defects build up and the solute redistribution, viz. RIS, reaches the steady state, the secondary defect formation starts inside the DLFZ and the width of DLFZ thus decreases as the irradiation continues.

We have shown that the formation energy of DLFZ is half of the radiation enhanced diffusion migration energy of solutes. This means that one can use the in-situ measurement of DLFZ in order to estimate the migration energy of the solute. There might be two advantages in the method: it can estimate the solute migration energy under irradiation:

1. At an intermediate temperature region, that is, the temperature range that vacancy and interstitial are both mobile and not superior to each other; if one kind defect is dominant, secondary defect clustering might occur.
2. By in-situ measurement and without evaluating the solute profiles; this unburdens the usual procedure for diffusion migration energy evaluation.

It should be remarked that further investigations on DLFZ formation might be necessary; for example, the dependence of damage rate, of different kinds of the irradiation particle, of grain boundary nature, and so on. Some evidences of such dependences on DLFZ formation have been recognized by the authors but will be discussed elsewhere.

Acknowledgements

The authors thank Dr N. Hashimoto and Mr N. Wake for their help in experimentation and discussions. S. W. would like to acknowledge Dr N.Q. Lam and Dr R.E. Stoller for the stimulating discussion.

References

[1] J.F. Bates, R.W. Powell, E.R. Gilbert, in: D. Kramer, H.R. Brager, J.S. Perrin (Eds.), Effects of Radiation on Materials, 10th Conf., ASTM STP 725, Amer. Soc. for Testing and Mater., Philadelphia, PA, 1980, p. 713.
[2] H. Gross, H.P. Fuchs, H.J. Lippert, W. Dambeitz, Nucl. Eng. Design 108 (1988) 433.
[3] H. Haninen, I. Aho-Mantila, in: G.J. Thues, J.R. Weeks (Eds.), Proc. 3rd Int. Symp. on Environmental Degradation of Materials in Nuclear Power System–Water Reactors, The Metal. Soc. of AIME, Warrendale, PA, 1988, p. 77.
[4] R.A. Johnson, N.Q. Lam, Phys. Rev. B 13 (1976) 4364.
[5] H. Wiedersich, P.R. Okamoto, N.Q. Lam, J. Nucl. Mater. 53 (1979) 98.
[6] P.R. Okamoto, L.E. Rehn, J. Nucl. Mater. 83 (1979) 2.
[7] S. Watanabe, N. Sakaguchi, N. Hashimoto, H. Takahashi, J. Nucl. Mater. 224 (1995) 158.
[8] R.B. Nicholson, Phase Transformations, Amer. Soc. for Metals, Metals Park, OH, 1968, p. 269.
[9] T.R. Anthony, in: J.W. Corbett, L.C. Ianniello (Eds.), Radiation-Induced Voids in Metals, U.S. Atomic Energy Commission, Albany, NY, 1972, p. 630.
[10] A.I. Ryazanov, G.A. Arutyunova, V.N. Sokursky, V.I. Chuev, J. Nucl. Mater. 135 (1985) 232.
[11] M. Suzuki, A. Fujimura, A. Sato, J. Nagakawa, N. Yamamoto, H. Shiraishi, Philos. Mag. A 64 (1991) 395; ibid 65 (1992) 1309.
[12] S. Watanabe, N. Sakaguchi, S. Mochizuki, H. Takahashi, Philos. Mag. Lett. 74 (1996) 351.
[13] N. Sakaguchi, S. Watanabe, H. Takahashi, J. Nucl. Mater. 239 (1996) 176.